Process Structure Property Relationships in Electron Beam Generated Cellular Materials

ROBERT W. GREER and GARTH L. WILKES*

Department of Chemical Engineering, Virginia Polytechnic Institute and State University, Blacksburg, Virginia 24061-0211

SYNOPSIS

Cellular materials were generated from radiation curable compositions of acrylated monomers and oligomers utilizing electron beam irradiation techniques. The relationships between the processing variables, the chemical compositions, and the final properties of these materials were examined. Two methods of producing these materials were compared. One process consists of frothing the radiation curable mixture before irradiation by a mixing technique and then casting the unpolymerized froth onto a substrate where it can be subsequently cured using electron beam radiation. Another process relies on a surfactant to stabilize the cellular structure before irradiation. It was found that the quality of the cellular structures produced by these techniques is highly dependent on the viscosity of the radiation curable mixture. A detailed outline of these processes with the resultant structures and properties of these cellular materials is presented along with comparison with other cellular material generation processes. © 1996 John Wiley & Sons, Inc.

INTRODUCTION

Previous work[1-5] has shown that it is possible to generate cellular materials by utilizing electron beam irradiation techniques. While there are several different methods of producing cellular materials in this fashion, all of the processes are based on a principal of prefrothing a radiation responsive mixture and then feeding this mixture into the electron beam radiation source, which cures the system. Some general advantages of using these techniques are having the ability to go from starting materials to final product in one step, and in principal, to do this in a continuous manner. Unfortunately, no systematic studies have been carried out to determine the effects of the type of different processes and the effect of processing variables on the structure property relationships for these materials.

* To whom correspondence should be addressed; e-mail gwilkes@vtvm1.cc.vt.edu

Journal of Applied Polymer Science, Vol. 62, 1115–1128 (1996)
 CCC 0021-8995/96/071115-14

Methods of Producing Cellular Materials by Electron Beam Irradiation Techniques

It is convenient to categorize the different processes as follows for the purposes of introducing this work.

Chemical Blowing Agent

Processes[6,7] that fall into this category rely on the addition of a compound to a polymer or a radiation curable monomer/oligomer blend. This compound decomposes upon irradiation and releases a gas that creates a cellular structure in the material by nucleation and growth of the cells.

Physical Blowing Agent

These processes[8,9] either utilize pressurized gas, which has saturated a polymer melt or radiation curable monomer/oligomer blend, or an agent, which releases a gas upon heating. The mixture is extruded (and preheated in the case of the thermally decomposable agent), which causes the system to expand into a cellular structure. Immediately after extrusion, the system is passed under the electron beam

that sets the cellular structure in place before collapse. Unlike the previous category, the system has the cellular structure prior to irradiation.

Prefroth Polymer by Mixing

This process[10] would be limited to polymers that crosslink in response to radiation, such as polybutadiene or polyisoprene. Also included in this category are systems that contain a polymer not normally thought of as a radiation crosslinker (such as PVC) and a reactive crosslinking plasticizer to crosslink the system, locking in the cellular structure, when irradiated. One would first melt the polymer, then mechanically entrain air, for example, by mixing with a dual high speed mixer. Once the system has generated sufficient froth, then one may extrude the froth into the electron beam, crosslink the system, and thereby produce the cellular material.

Prefroth Monomer by Mixing

There are actually two separate techniques[11,12] that start from a monomer. The first technique, which will be termed the surfactant method, relies on a surfactant and a low molecular weight, low viscosity radiation curable monomer. First air is blown through the mixture of the surfactant and the monomer, which generates a froth. This froth is then extruded to a fixed thickness and passed through the electron beam, which locks in the cellular structure. The key to this technique is that the surfactant stabilizes the cellular structure prior to irradiation.

The second technique in this category is the principal focus of this work. It does not rely on a surfactant, but instead is similar to the prefroth polymer by mixing process. Starting with a high viscosity system of a radiation curable oligomer or a monomer/oligomer blend, one froths the system with a dual high speed mixer, then extrudes the froth into the electron beam for curing. One of the significant differences between the techniques is what "stabilizes" the cellular structure prior to irradiation; either a surfactant or the viscosity of the mixture.

As one can see from the above descriptions that much of this previous work relied on the use of surfactants or blowing agents, which make the process more complex and expensive. In this work, emphasis was placed on the generation of cellular materials from radiation curable materials without the use of heat, surfactant, or blowing agents. This technique relies on a sufficient viscosity to hold the cellular structure in place after it has been mixed as opposed to using a surfactant that relies on surface tension to stabilize the cellular structure in place before curing. Details of this viscosity requirement were studied in detail. In addition, it is possible to polymerize into the material blends of radiation curable species with different properties in order to custom tailor the material for a specific range of applications (e.g., high or low glass transition temperature, T_g, high modulus, etc.)

Although it is possible to synthesize surfactants that have radiation curable functionality, and a few radiation curable surfactants are commercially available, common surfactants do not have radiation responsive groups (e.g., allylic groups). Therefore, most of the previous work relied on surfactants that do not respond to a radiation cure and become part of the structure by reacting into the network.[13]

The advantages of the mixing process over the other techniques outlined previously are that no preheating is involved and no prepolymerization of the mixture before irradiation is required. In addition, no blowing agent (chemical or physical) and no surfactant are required for producing the cellular structure. While this technique (termed mixing process) was the primary focus of this work, it is important to contrast this approach with the technique utilizing a surfactant (termed surfactant process). This is because of the importance of the viscosity of the radiation curable mixture. It is this processing variable that determines which process is appropriate.

It is the purpose of this work to examine what process–structure–property relationships exist between these materials. It is hoped that this can provide additional information about understanding the resulting cellular materials and the potential applications for them.

EXPERIMENTAL

Reactant Materials and Their Characterization

Acrylated functionalized materials were generously supplied by Radcure, a manufacturer of electron beam and UV curable coatings, under the commercial names of β-CEA, TMPTA, HDODA, Ebecryl 4827, and Ebecryl 1701. The structures of these compounds are outlined in Figure 1. It was desirable to compare monomers of different functionality in this work; therefore, a monoacrylate (β-CEA), diacrylate (HDODA), and a triacrylate (TMPTA) were selected. Ebecryl 4827 and 1701 are acrylated urethane oligomers of unknown structure, but for the

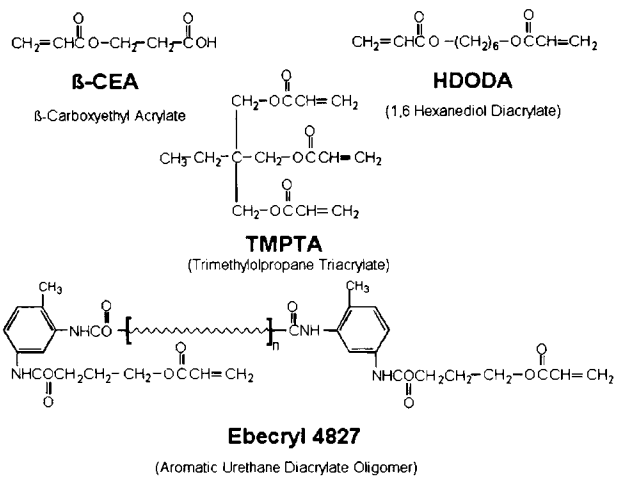

Figure 1 Structures of the acrylate materials used in this study.

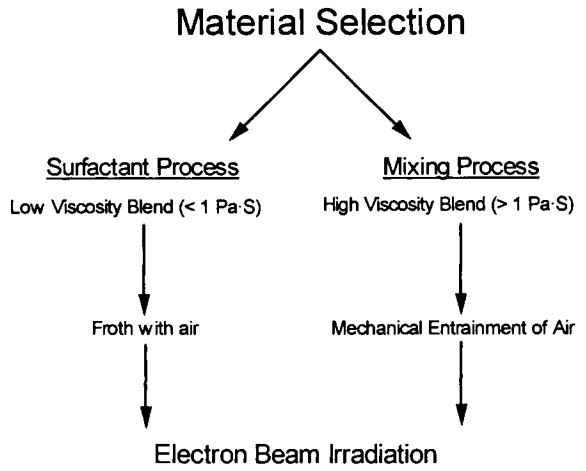

Figure 2 Qualitative outline of the electron beam cellular material generation process involving the mixing technique.

purpose of this work, the most noted difference is their molecular weight and viscosity. Fluorochemical surfactant was obtained from 3M Corp. under the trade name of FC-430. FC-430 was selected because it was utilized in previous work[14] involving the surfactant process with monomers similar to the ones shown in Figure 1.

Thin films of the monomers and oligomers were cast using a scalpel on glass and cured in an ESI Electrocurtain 175-keV electron beam accelerator using doses of 0.625, 1.25, 2.5, 5, 10, 20, and 40 Mrad. Two samples were irradiated to higher doses. It should be noted that typical doses seen in industrial applications range up to 20 Mrad, with 2–10 Mrad being typical for most curing operations. However for this work, higher dose experiments were performed in view of our interest regarding extent of cure. They were then characterized according to their cured T_g as a function of dose using differential scanning calorimetry (DSC) on a Seiko model 220C. These measurements were combined with FTIR results (using the same doses) to aid in analysis of dose optimization. FTIR work was performed using a Nicolet 510 FTIR spectrometer.

Viscosity measurements of the reactants and their mixtures were determined at 25°C using a Bohlin CS rheometer with cone and plate geometry. Viscosity results are summarized in Table I. For the range of shear rates with which these materials were tested (up to 661 s^{-1}), the data indicated Newtonian behavior. Due to instrumentation limitations on the upper limit of generated shear stress, higher shear rates were not accessible for the oligomers.

Cellular Material Preparation

Figure 2 outlines the process used to produce the cellular materials. First, materials were selected based on their viscosity and *cured* T_g. This step is critical as it largely determines the final material properties. For example, if a stiff structural material

Table I Summary of Rheological Properties of Reactive Chemicals Used in This Study

Material Name	Description	ρ (g/mL) at 25°C	MW (g/mol)	Shear Rates Tested (s^{-1})	Viscosity (Pa s)
β-CEA	β-Carboxyethyl acrylate	1.21	144	2.89–661	0.20
HDODA	1,6 Hexanediol diacrylate	1.02	226	2.89–661	0.0054
TMPTA	Trimethylolpropane triacrylate	1.10	296	0.888–99.90	0.094
Ebecryl 4827	Aromatic urethane diacrylate oligomer	1.11	1,500	0.106–2.892	269.0
Ebecryl 1701	Acrylated acrylic oligomer	1.10	27,000	0.0837–1.125	1,200

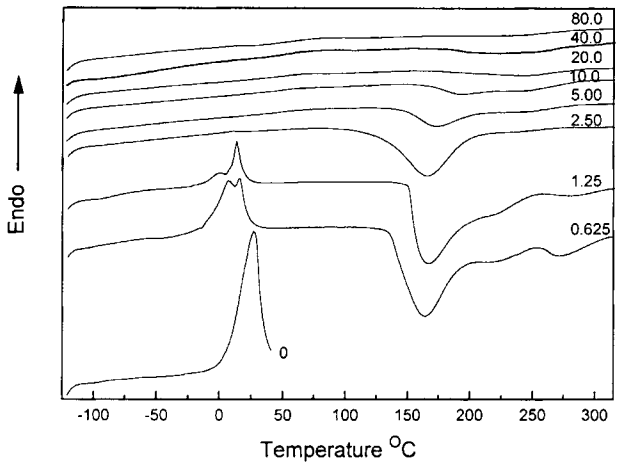

Figure 3 DSC for HDODA as a function of dose. Dosage values are in megarads (Mrad).

is desired, then more rigid, high T_g (upon curing) materials should be selected; however, if a more flexible cellular material is desired, then reactant materials having a low T_g (upon curing) should be selected. The systems were then processed depending on the viscosity of the selected components. For the case of the cellular materials produced via the mixing process, the oligomers and monomers were combined with a dual mixer/blender at high speed until such time as a stable froth was generated. Then, the froth was cast on a substrate with a scalpel set at a fixed height. The casting thickness was set at 16–20 mil and determined roughly as 4 times the uniform depth of penetration for the Energy Sciences Inc. Electrocurtain 175-keV electron beam accelerator (4 mil). The "average" froth generated for this process had approximately 50% air; therefore, a casting thickness of ca. 8 mil would allow sufficient exposure to assume uniform exposure. However, to produce thicker samples, the froth was cast at 16 mil and irradiated on both sides.

Because of the depth–dose profile for our electron beam unit, the first pass was typically sufficient to solidify the cellular material. The second pass on the other side assured a relatively even cure. For comparative purposes, another type of cellular material was generated via the above-mentioned surfactant method (also outlined in Fig. 2) from a low viscosity mixture of only monomers with a small amount of the acrylated fluorochemical surfactant (Fluorad FC-430). In this case the surfactant was added to a monomer and then nitrogen was bubbled through the mixture. The froth was then poured onto a petri dish and immediately cured in the electron beam accelerator using the dual pass method described above.

Cellular Material Characterization

Scanning electron microscopy (SEM) studies of the resulting cellular materials were performed using a Cambridge Instruments Ltd. Stereoscan 200 microscope. Mechanical testing in tension was performed at ambient conditions on an Instron model 1122. The strain rate used for all tensile testing was 0.1 mm/min. Dogbone samples, 10 × 2.75 mm, were cut for all specimens. Sample thickness varied from about 3 mil for the films and about 20 mil for the cellular materials.

RESULTS AND DISCUSSION

Level of Cure for a Given Dose

The goal of this analysis was to determine the range of T_gs the cured materials had and, therefore, aid in selecting materials for stiff structural type applications or more flexible applications. In addition, it was desirable to know what the sensitivity to these materials was to a given dose, and to determine what percent residual double bonds exist in the materials because uncured acrylate groups would contribute to network defects that, in turn, would influence mechanical properties. The additional concern for acrylate monomer diffusing out of these materials also motivated these experiments. Finally, because of the low dose desired from a practical and environmental viewpoint, dose–cure level optimization was required. This analysis was performed utilizing FTIR and DSC as a function of dose, starting with a dose of 0.625 Mrad and doubling the dose up to 20–80 Mrad, depending on the material.

Figures 3 and 4 show DSC scans as a function of dose for the single components of HDODA and TMPTA. Similar trends were found for β-CEA and Ebecryl-4827. The figures show DSC traces for doses from 0 to 40+ Mrad. The 0-Mrad (uncured) materials were only run up to room temperature to avoid damage to the DSC cell from a curing reaction. What is shown in each figure for the uncured system is one of two transitions (T_g or melt temperature, T_m). Next, each transition rises in temperature as the dose increases. Finally, (at high doses) the transitions level off or disappear at some point. While pinpointing the T_g for these materials is difficult, the two monomers shown (HDODA and TMPTA)

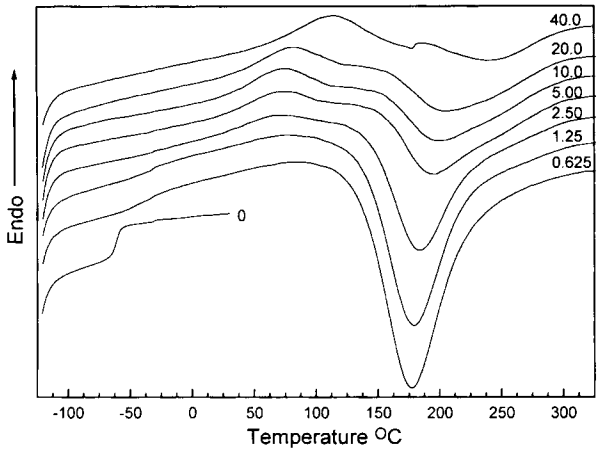

Figure 4 DSC scans for TMPTA as a function of dose. Dosage values are in megarads (Mrad).

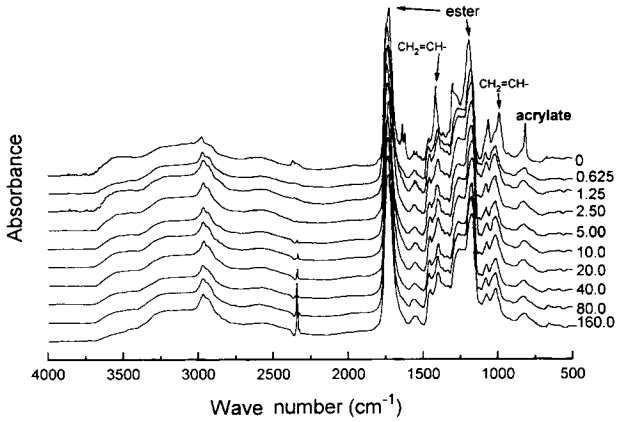

Figure 5 β-CEA FTIR scans as a function of dose. Numbers indicate total dose for each sample in megarads (Mrads).

both had T_gs in excess of 100°C while the oligomer's T_g was approximately −25°C. The difficulty in pinpointing a fully cured T_g of a material arises because, for a high functionality monomer, the signal from the DSC becomes very "flat" and it is hard to observe a change in heat capacity, which is typical for crosslinked systems. At lower doses, a T_g may be observable; but one has to recognize the fact that there may be residual unreacted monomer present that is plasticizing the system, which would lower the T_g as measured. In Figure 3 data for HDODA is shown. A melting point occurs at approximately 0°C for the sample with no cure (0 Mrad). For the next two curves, which result for the 0.625 and 1.25 Mrad dosage levels, the melting point is still observable, indicating residual monomer is present. For these two curves, a reaction exotherm occurs at 125°C. This reaction exotherm can only typically occur if the system has attained the cooperative segmental backbone motion associated with T_g. Increasing the dose causes this exotherm to disappear until only a flat line is observed in the DSC. One can see the trend of the T_gs of the lower dose samples to "climb" and then disappear, which is typical for systems such as these. If one assumes the same trend of T_g continues with respect to dose, one can approximate the T_g for this material at 225 ± 25°C. Using a similar analysis for TMPTA, one can observe the same trend in Figure 4; however, the curves for the "high" doses do not flatten out as they did with HDODA. Assuming this trend continues, a *fully cured* sample of TMPTA should have a fully cured T_g around 300°C+. A full cure, defined as every double bond reacting as part of the network, is not realistic, because with $f = 6$, a full cure would never happen at or close to room temperature due to time temperature transformation (TTT) effects and the high cured T_g of TMPTA. The monoacrylate sample, β-CEA, showed a T_g that did not increase with dose. It is believed that this is due to low functionality and lack of any potential crosslinking groups other than one acrylate group per molecule. Finally, the oligomer showed a T_g (ca. −25°C) that did not significantly increase with dose.

Figures 5–8 show data from the FTIR analysis. This analysis was coupled with DSC, primarily to follow residual double bond content as a function of dose. The acrylate peak at 810 cm^{-1} was used for this analysis and normalized on the ester peak at ca. 1750 cm^{-1}. Samples of each monomer or oligomer were coated on a KBr pellet and a scan was taken. To assure that quantitative work could be performed on the scans, the coating on the KBr pellet was made thin enough so that no absorbance peak was above

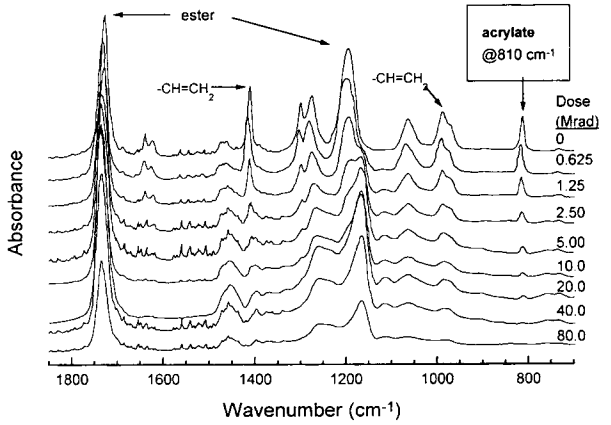

Figure 6 FTIR scans for HDODA as a function of dose.

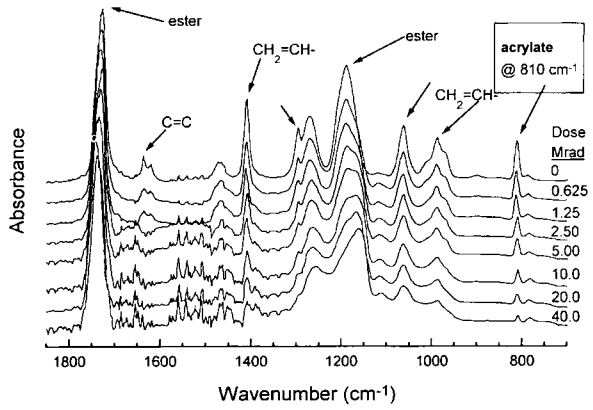

Figure 7 FTIR scans for TMPTA as a function of dose.

1.0. The same sample was then irradiated at 0.625 Mrad, then scanned in the FTIR, and the dose increased (doubling each time) until a total dose of 40–160 Mrad was reached. Higher doses were given to some samples to see if any further reduction in the acrylate peak or other reactions took place.

Figure 5 shows data for β-CEA. The entire spectrum is shown in this figure to illustrate that in these materials, the significant changes occur primarily in the fingerprint region from about 600 to 1900 cm^{-1}. Like the oligomers, increasing dose beyond a few megarad did not significantly decrease the acrylate peak.

This material was particularly unique in that increasing the dose continued to quickly reduce the number of residual double bonds present, even though the exotherm in the DSC trace appeared to disappear at ca. 20 Mrad. Figure 6 shows that at 20 Mrad there is still a visible acrylate peak in HDODA. The triacrylate material (TMPTA) showed both residual double bonds and a significant DSC exotherm at 20 Mrad (see Fig. 4). Both oligomers showed an immediate reduction with very low doses and then no significant reduction in double bonds with increasing dose.

The FTIR analysis is summarized in Figure 8. Note that in all the materials there are significant unreacted groups at 20 Mrad; however, this does not necessarily mean that these materials contain unreacted groups that are free to diffuse out of the bulk sample. For example, a triacrylate molecule would have a very high probability of reacting with another triacrylate group and becoming part of the network (gel fraction). However, there could easily be unreacted groups in that same network that would contribute to residual double bonds and DSC exotherm from thermolysis, yet not allow diffusion of this molecule out of the bulk sample. A dose of 20 Mrad was used to cure the cellular materials for both the surfactant and the mixing methods. This dose was chosen after a careful analysis of the radiation cure response of the materials used in the study. Industrial applications typically rely on doses on the order of 2–10 Mrad for curing and crosslinking samples; however, a higher dose was chosen to err on the side of a complete cure vs. optimizing energy usage in an industrial process.

Processing Variables

The most important processing variable is the mixture viscosity, which can be controlled by altering mixture composition and, in principal, altering temperature. In this work temperature is not considered a significant processing variable because excessive heating (to reduce viscosity) can cure the material. However, if one takes the possibility of a thermal cure into consideration, some limited heating would be possible to reduce the system viscosity. In the case where a higher viscosity would be desired, cooling the reactant mixture could also be considered. To better understand the rheological process–property variables, a series of optimization experiments were performed.

Rheological testing was performed on a Bohlin CS rheometer using a cone and plate configuration. Figures 9 and 10 show diluent effects on the viscosity of Ebecryl 1701 and 4827. One will note deviation from the "straight line" rule of mixtures approach for Ebecryl 1701 and HDODA in Figure 10. The rule of mixtures is a simple concept that with respect to

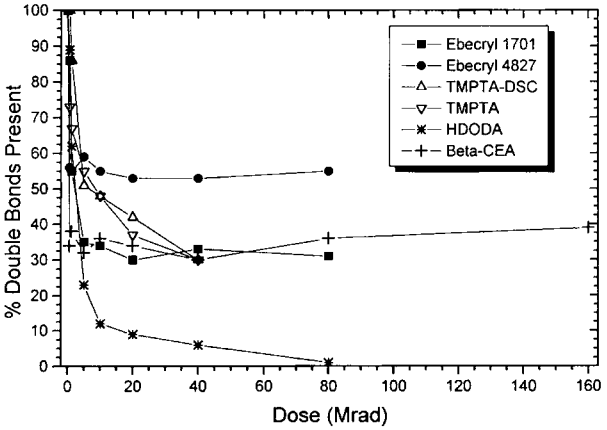

Figure 8 Summary of normalized acrylate peak response for all materials. Also included (for comparative purposes) is the reduction in DSC peak exotherm for TMPTA triacrylate.

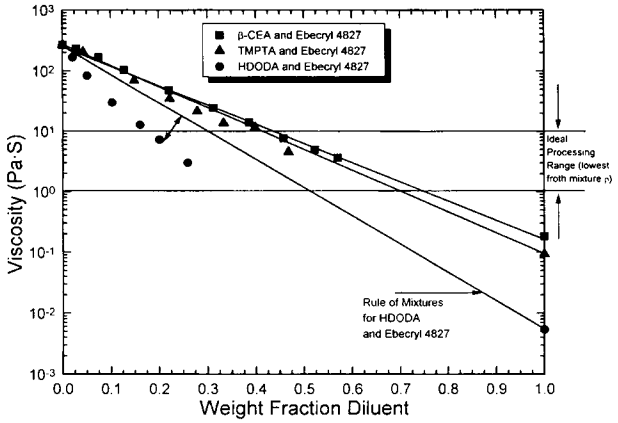

Figure 9 Viscosity at 25°C as a function of composition for β-CEA, HDODA, and TMPTA monomers with Ebecryl 4827 oligomer. Straight lines are drawn for the rule of mixtures using the viscosities of the pure components for intercepts.

a mixture "property," a blend of substances will have a "property," that is, a linear combination of the pure components. Of course, the exceptions to this are more common than the rule. The rule of mixtures applied to viscosity yields[15]

$$f(\eta_m)_L = \sum_i \chi_i f(\eta_i)_L \qquad (1)$$

where η_m is the viscosity of the mixture, η_i is the viscosity of the individual component, and χ_i is the volume fraction of component I. Many modifications of this theory exist. Lobe[16] modified the above equation with an exponential term containing an adjustable characteristic viscosity parameter to deal with deviations from the rule of mixtures theory. Data from the HDODA and Ebecryl 1701 experiments were fitted to the equation and the results are shown in Figure 10. The form of the equation used was

$$\nu_m = \sum_{i=1}^{n} \Phi_i \nu_i \exp\left(\sum_{j=1}^{n} \frac{\alpha_i \Phi_j}{RT}\right) \quad j \neq i \qquad (2)$$

where ν is the kinematic viscosity (η/ρ) (cSt), F_j is the volume fraction of component j, α_j is the characteristic viscosity parameter for component j in the mixture (cal/g mol K), R is the gas constant (=1.987 cal/g mol K), and T is the temperature (K).

All materials tested showed some level of deviation from the rule of mixtures for viscosity, with HDODA showing the strongest deviation and TMPTA and β-CEA showing more mild deviation (see Fig. 9) in blends with Ebecryl 4827. HDODA was also tested in 14 different compositions with Ebecryl 1701 and showed the same strong deviation from this rule (see Fig. 10).

The consequence of these deviations results in a more difficult process optimization procedure in that prediction of mixture viscosities is more difficult without the full curve. For example, if the desired mixture viscosity for a blend of HDODA and Ebecryl 1701 is 1.0 PaS, then based on the straight line approach one would use a composition of approximately 58% HDODA. In reality this composition would give a mixture viscosity of approximately 0.225 PaS. This deviation has a dramatic effect on the cellular material generation as will soon be shown.

As discussed in the previous section, the primary method of lowering a mixture viscosity into the appropriate range where processing is possible is by adding a reactive diluent. While viscosity is also a function of temperature, it is important to note that heating these types of monomers and oligomers could result in undesirable reactions from thermally induced curing. However, slight limited heating could be possible if one is careful to avoid thermal curing. More dramatic heating could be accomplished if one raised the temperature of the froth mixture immediately before irradiation. Raising a mixture viscosity could be accomplished by reducing the amount of reactive diluent or cooling the mixture. Therefore, adding low viscosity diluents to high viscosity oligomers to lower mixture viscosity is the method primarily relied upon to control mixture viscosity. Figure 11 shows qualitatively the role viscosity plays in the two processes compared in terms

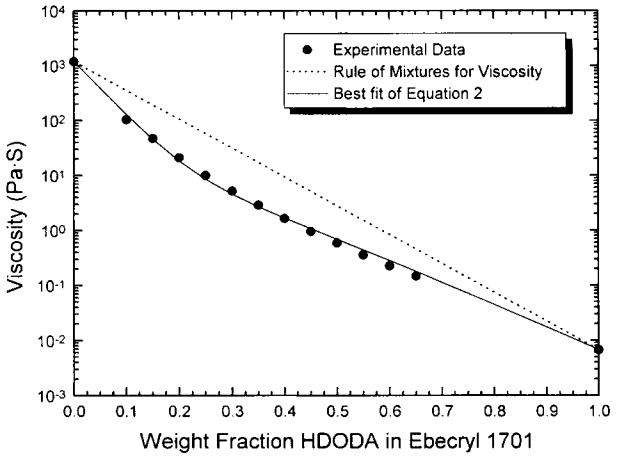

Figure 10 Viscosity at 25°C as a function of diluent concentration for HDODA and Ebecryl 1701.

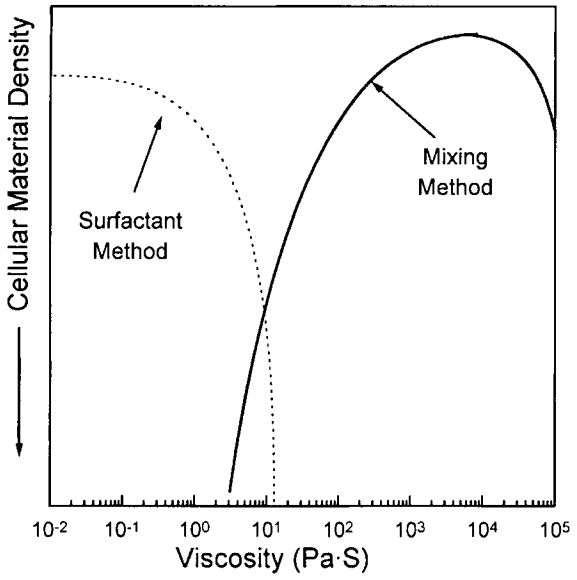

Figure 11 Generalized qualitative comparison of the effective processing ranges for the two cellular material generation processes.

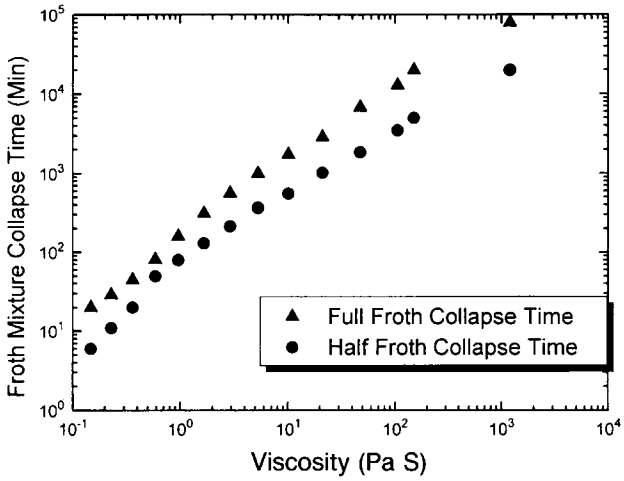

Figure 12 Froth collapse time at 25°C in minutes as a function of mixture viscosity. Data for the system HDODA and Ebecryl 1701. In the case of shear thinning behavior, viscosities shown are the 0 shear viscosities.

of the viscosity ranges over which they effectively operate. The first curve is a qualitative optimization line for the process involving the surfactant, and the second line (in the higher viscosity range) is a qualitative optimization line for the process involving mixing a higher viscosity composition. Attempts have been made to lower this processing limit below the 1 Pa s barrier because it would be desirable to operate the mixing process in a lower viscosity range without the use of a surfactant. It was found that the frothing process utilizing the surfactant had an upper limit of approximately 1 Pa s where, at which point, it became difficult to generate the froth due to the higher viscosity. As a result the investigation was directed at avoiding this problem by generating the froth by another technique and at the same time eliminating the use of the surfactant. The surfactant did not have any radiation curable functionality; therefore, it did not become part of the material after cure and could diffuse out at a later time. It was observed that mechanical mixing would produce a froth; however, the mixture was required to be above a certain lower limit of viscosity (also approximately 1 Pa s) for the mixing technique to work and produce a sufficiently stable froth.

While Figure 11 shows the effect qualitatively, Figures 12 and 13 show this effect more quantitatively. Figure 12 shows froth collapse time data as a function of mixture viscosity. The collapse time increases dramatically with small increases in mixture viscosity; while one might initially assume that this is a desirable effect. Figure 13 shows mixture density as a function of viscosity with a minimum in the range of 1–10 Pa s. Coupling Figures 12 and 13 results in a quantitative version of the right half (for the mixing technique) of Figure 11.

If one only considered collapse time as a process optimization variable, then one would assume that a higher viscosity is better in all cases. However, as shown in Figure 13, the mixture density clearly goes through a minimum value in the range of 1–10 Pa s. As implied in Figure 12, below ca. 1 Pa s, there will not be enough time to cure the material before it collapses using the mixing method. This may be

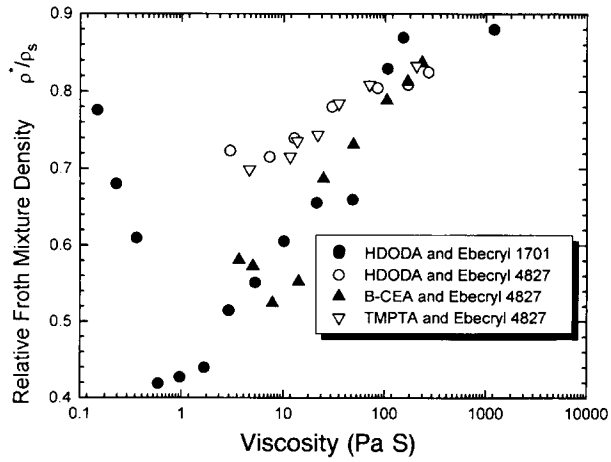

Figure 13 Relative mixture density at 25°C as a function of mixture viscosity for the compositions tested.

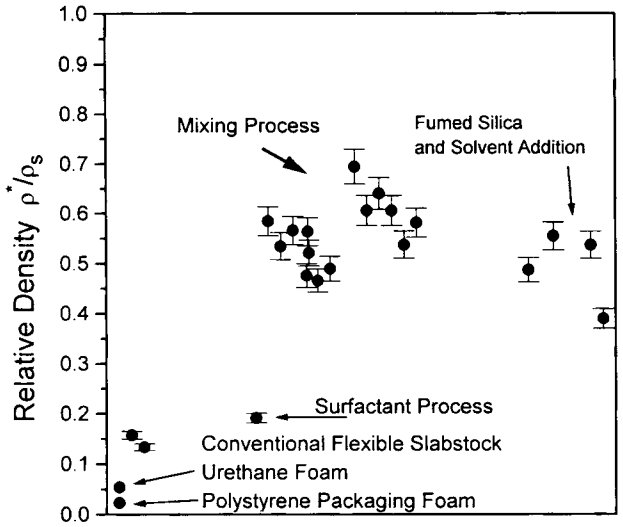

Figure 14 Density data for different samples determined by measuring the weight of the final product and dividing by the volume.

confirmed by observing the collapse time data in Figure 12. At this point, a surfactant must be utilized to support the froth until it can be cured in the electron beam radiation source. Alternatively, the process line speed could be increased to reduce the time from froth extrusion to irradiation. As shown in Figure 13 the mixture density starts to increase in this same range of 1 Pa s. At higher viscosities (and collapse times), the power of the mixer becomes the limiting factor in generating a low density froth (although, as mentioned before, limited heating to reduce viscosity would also be possible). No comparisons among different power mixers were made, and at these higher viscosities (100 Pa s and higher) much torque is required of the motor to even stir the mixture. Much lower revolutions are the result of this strain, which leads to less entrained air and a higher froth density.

While froth mixture density appears to be the most logical or convenient method for calculating the density of the final product, due to shrinkage and skin affects on these materials, densities were recalculated using a standard weight of a sample divided by its volume. A micrometer was used to measure five samples cut from a standard die and the results are shown in Figure 14. Figure 14 shows densities of a sampling of electron beam generated cellular materials produced by the mixing technique and the surfactant technique along with some commercially available low density foams. Relative density is defined as the density of the cellular material divided by the density of the respective solid.

It is interesting to note that although these cellular materials are higher in relative density than either a typical flexible slabstock urethane foam or polystyrene packaging foams shown in the graph, they appear at least to have densities for closed cell materials that are in the range of what might be thought of as a "theoretical minimum." That is, if one assumes that the cells formed are spherical in nature and treats the density as a packing factor for spheres, appreciation is gained for these materials. For example, the packing factor for random loose uniform size spheres is 0.601, which would correlate to a relative density of 0.399. Hexagonal close packing gives a packing factor of 0.7405, or a relative density of 0.2595. To be fair, the cells in these materials are not discrete and many are connected, which would promote a lower density due to fewer cell walls. However, the overall cellular material morphology is one of closed, spherical cells.

SEM

Figures 15–17 show the type of cellular structure that is generated by the mixing technique. The cells tend to be closed cell in nature and range from 0.02 to 0.1 mm in size. These materials can be flexible due to the low cure T_g oligomers that can be used in their production. Relative density ranges for these cellular materials are 0.38–0.70. Figure 18 shows a cellular material generated by the technique involving the surfactant. This process produces a rigid,

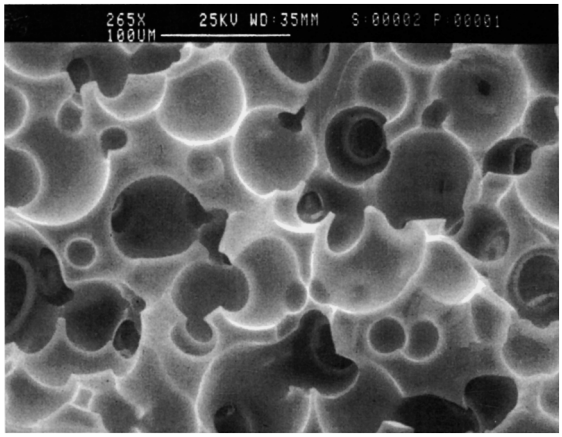

Figure 15 SEM of a blend of 75% Ebecryl 4827 and 25% β-CEA. The system was mixed and then cured as described in Figure 2. Scale bar = 0.1 mm.

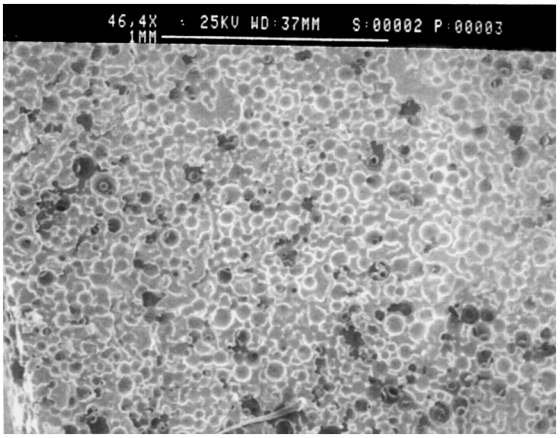

Figure 16 SEM of same material as in Figure 15. Scale bar = 1 mm.

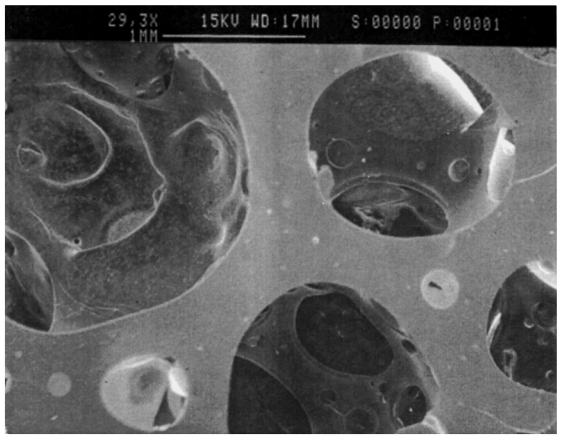

Figure 18 SEM of material produced using 3% Fluorad FC-430 fluorochemical surfactant and 97% TMPTA.

open cell material with relative densities in the range of 0.2. The cells in this material are much larger than obtained from the mechanical mixing process, tending to range from 0.3 to 2 mm in size. There is also much lower uniformity in the cell sizes for these materials. For this process to work, low viscosity materials (low molecular weight) are required that typically cure to form high T_g systems (e.g., low molecular weight diacrylates and triacrylates). Therefore, these materials tend to be rigid and hence these would be more useful in structural applications. The reactive materials that do have the low cured T_g (the oligomers) have viscosities that are too high to be used in this process because it is impossible to bubble and froth such a mixture. As mentioned previously, heating the mixture might be possible to lower the viscosity, provided the heating process did not thermally cure the mixture prematurely.

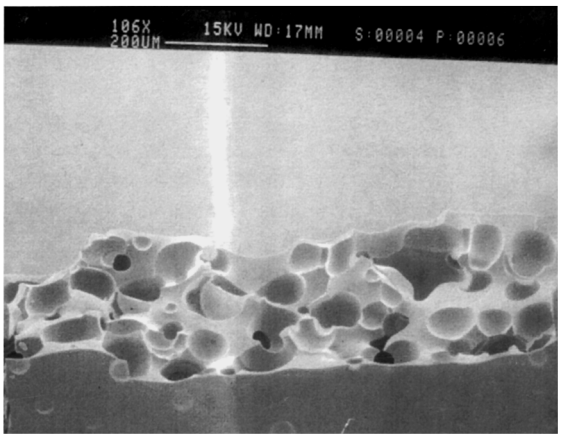

Figure 17 SEM of cellular material produced by the mixing technique showing edge view perspective.

Mechanical Properties

To illustrate the ability to tailor the modulus of the cellular material by increasing the content of a reactive diluent group, a systematic series of experiments were carried out. Ebecryl 4827 oligomer was selected for blending monoacrylate (β-CEA), diacrylate (HDODA), and triacrylate (TMPTA) and measuring tensile modulus as a function of monomer concentration. Both films and cellular materials were produced at each selected composition for comparison with theories that correlate these properties with density. Figures 19–25 show the results of these experiments. Depending on the chemistry of the diluent, very different changes in the tensile modulus of these materials result. Figures 19–21 illustrate the ability to systematically modify tensile

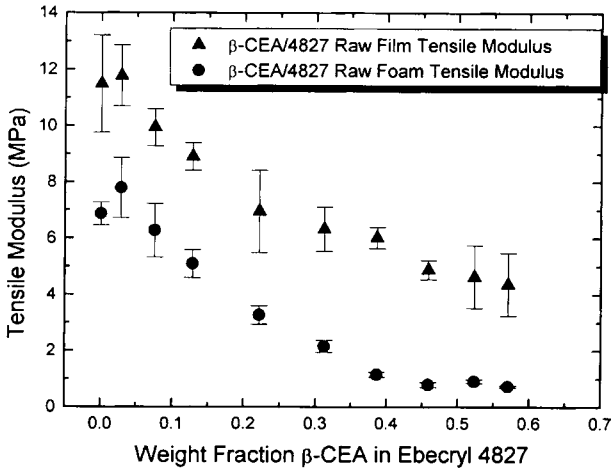

Figure 19 Film and cellular material tensile modulus as a function of weight fraction β-CEA.

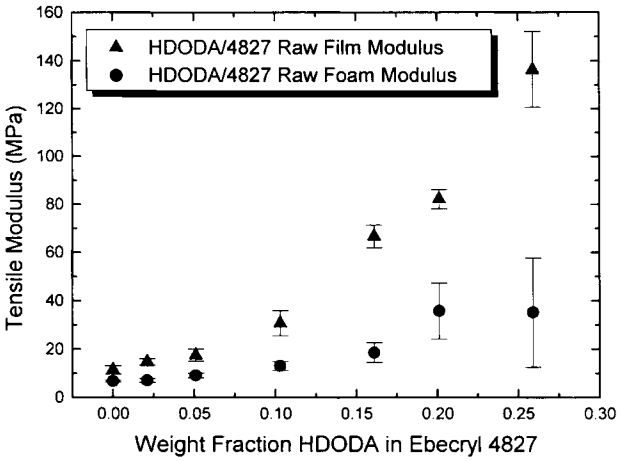

Figure 20 Film and cellular material tensile modulus as a function of weight fraction HDODA in the blend.

modulus by the addition of a reactive diluent. In these figures the modulus displayed is the actual tensile modulus of the material as measured.

Stress and strain at break analysis was performed on the same series of materials as in the previous three figures. For a material in which the modulus increases as a function of decreasing molecular weight between crosslinks, one would expect the stress at break to increase with increasing modulus and the strain at break to decrease with increasing modulus. In the series of experiments involving β-CEA monoacrylate, the tensile modulus decreased with increasing β-CEA content. For this series, the stress and strain at break showed the opposite trend (within experimental error) as would be expected.

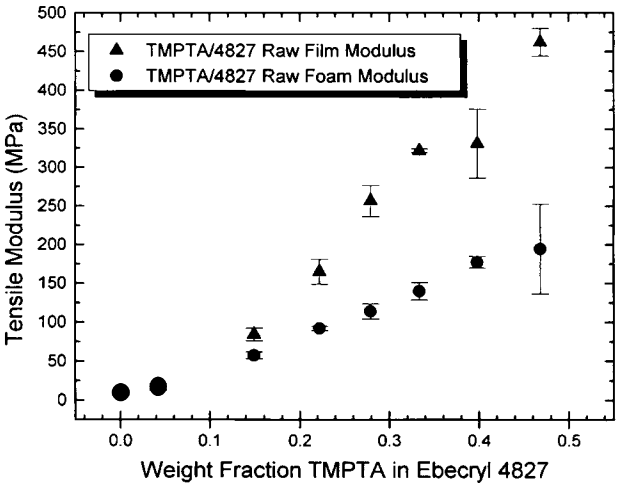

Figure 21 Film and cellular material tensile modulus as a function of weight fraction TMPTA in the blend.

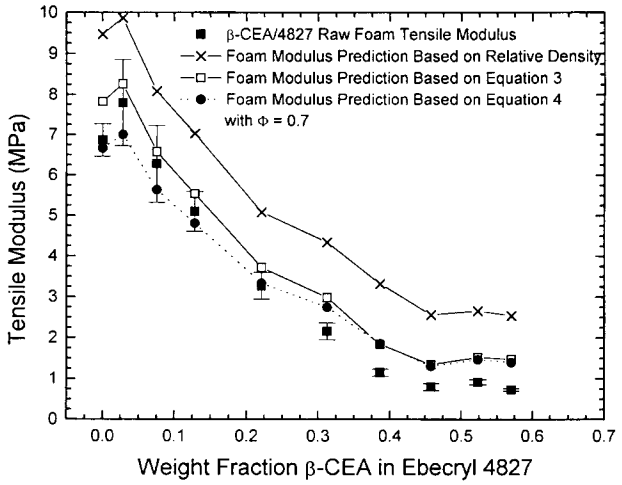

Figure 22 Theoretical tensile modulus prediction by various theories as compared with experimental data for β-CEA monoacrylate and Ebecryl 4827.

It is believed that β-CEA acts to cap the ends of Ebecryl 4827 oligomer, which would reduce the molecular weight between crosslinks and produce a looser network. Because β-CEA has a functionality of two, at best it can only form linear species (assuming no other crosslinking reactions take place other than via the acrylate group). This reduces the chances of linking up unreacted oligomer acrylate end groups with the network and basically leaves network defects. This must be taken into account in optimizing the process as increasing β-CEA content lowers the cellular material density but at the same time lowers the tensile modulus and decreases the stress at break.

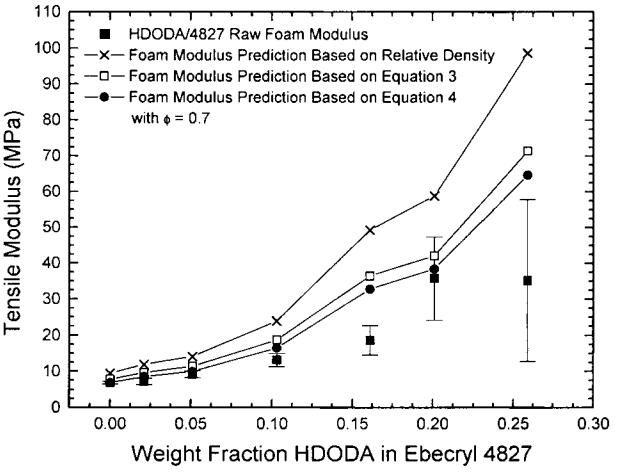

Figure 23 Theoretical tensile modulus prediction by various theories as compared with experimental data for HDODA diacrylate and Ebecryl 4827.

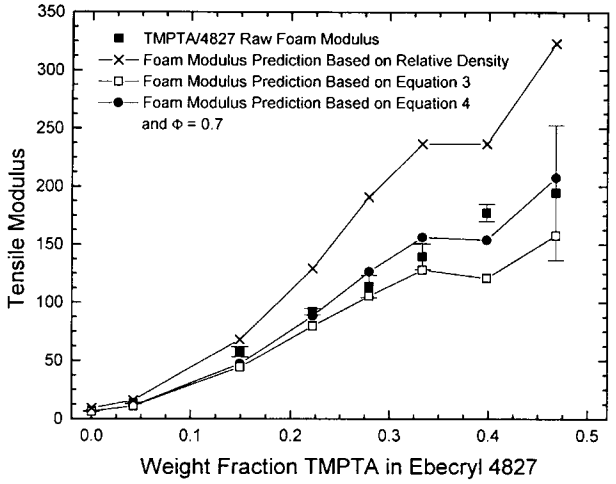

Figure 24 Theoretical tensile modulus prediction by various theories as compared with experimental data for TMPTA monoacrylate and Ebecryl 4827.

Gibson and Ashby[17] provide an excellent analysis of closed and open cell materials. Their approach takes into account the density of the cellular material as an important factor in comparing the tensile moduli of different materials. They found the following equations to be adequate for modeling the tensile moduli of cellular materials. For open cell foams,

$$\frac{E^*}{E_s} = \left(\frac{\rho^*}{\rho_s}\right)^2 \tag{3}$$

where E^*/E_s is defined as the relative modulus (the modulus of the foam divided by the solid material) and ρ^*/ρ_s is defined as the relative density of the cellular material.

For closed cell foams, the gas pressure in the cells, the composition of the cell faces, and Poisson's ratio of the material must be taken into account. Experimental data from Gibson and Ashby[17] correlate well with the following equation:

$$\frac{E^*}{E_s} \approx \Phi^2\left(\frac{\rho^*}{\rho_s}\right)^2 + (1-\Phi)\frac{\rho^*}{\rho_s} + \frac{\rho_0(1-2\nu^*)}{E_s\left(1-\frac{\rho^*}{\rho_s}\right)} \tag{4}$$

where Φ is the variable fraction of solid in the cell faces, p_0 is the gas pressure in the cells (assumed to be 0.1 MPa), and ν^* is the Poisson's ratio of the cellular material (assumed to be 1/3 in our first-order calculations).

Figures 22–25 compare experimental data with these two theories. In Figures 22–24 data for the relative froth mixture density was used along with the modulus of the film to predict the modulus of the cellular material. Actual data for the cellular material modulus is displayed for comparative purposes. For Gibson and Ashby's closed cell equation,[17] a value of $\Phi = 0.7$ was used for all three systems. As can be seen from Figures 22–24 normalizing a cellular material modulus on density deviates strongly from actual data. Normalizing on density squared shows a better approximation and the closed cell equation shows the best correlation for experimental data. In Figure 25 experimental data are fit to eq. (4). The equation provided a reasonable fit for blends with β-CEA and TMPTA; however, the HDODA blends did not fit well. Possible explanations for this deviation can be found in the struts of the cells in these materials. They are not typical for closed cell materials as would be observed in polystyrene, for example. In addition, in many places in this material, no struts are observed at all.

Other Applications: Layered-Laminate Materials

Interest in producing a material that had a core cellular structure with a skin of a solid material generated two brief experiments involving curing a froth layered with a film of either polyethylene or nitrile rubber. The primary goal of this experiment was to show that materials such as these could be produced. Motivations for such materials could be

- to have a material that had a lower bulk density than without the cellular core;
- to have a lower density structural material;

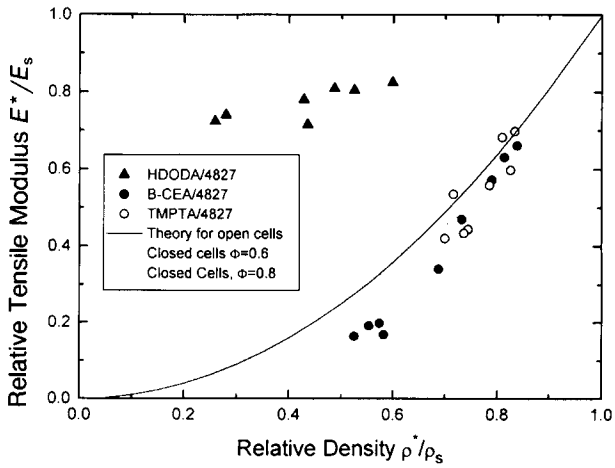

Figure 25 Relative modulus vs. relative density for all materials.

- to have a material with an integral skin, but of lower density; and
- to improve combined properties of the materials such as toughness, tear resistance, and damping.

Figures 26 and 27 show scanning electron micrographs of the materials prepared. The thickness of the films was approximately 1 mil for the polyethylene (PE) film and 3 mil for the nitrile–butadiene (NBR) rubber film. A froth composition of 50/50 β-CEA and Ebecryl 4827 was used to produce the cellular structure. The most notable difference between the two materials was the adhesion between the film material and the cellular material. Not surprisingly, the PE film had relatively poor adhesive properties, while the NBR rubber material was significantly better, as expected.

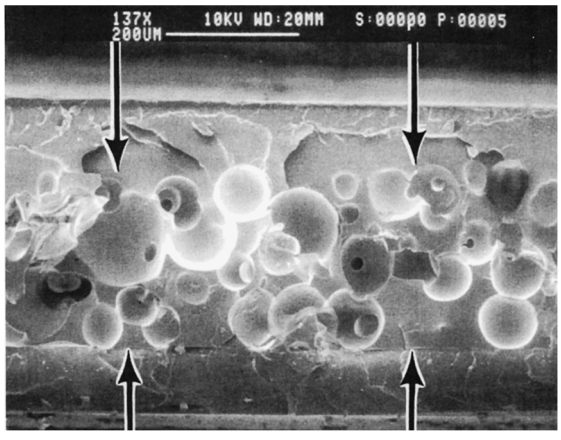

Figure 26 Scanning electron micrograph of layered material utilizing a nitrile rubber skin with an electron beam generated cellular material core with a composition of 50% β-CEA and 50% Ebecryl 4827.

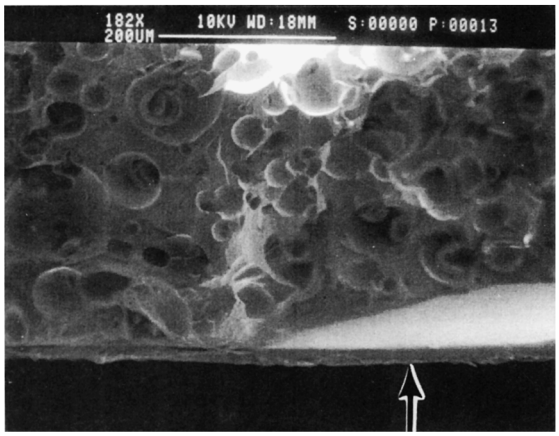

Figure 27 Scanning electron micrograph of layered material utilizing a polyethylene skin with an electron beam generated cellular material core with a composition of 50% β-CEA and 50% Ebecryl 4827. "Shelf" appearance on the right side of this material shows the poor adhesion the core material had to the polyethylene skin.

CONCLUSIONS

A technique was developed that produces closed cell materials by a mixing technique followed by a radiation cure from a radiation curable composition of a suitable viscosity. This process eliminates the need for surfactant to be used as well as heat and/or blowing agents. Comparison of this process with a technique involving a surfactant shows much smaller cell size as well as a tighter control over cell size distribution. Changes in process and cellular material property can be accomplished in the mixing process through the addition of reactive diluents that change the mixture viscosity. Addition of a triacrylate or diacrylate to a mixture of an aromatic urethane diacrylate oligomer increases the modulus of the cellular material while addition of a monoacrylate decreases the modulus but increases the elongation at break. Modeling of these mechanical properties with the Gibson and Ashby[17] analysis show the same trends but do not fit well, possibly due to differences in cell strut structure in these materials. Any addition of reactive monomers to radiation oligomers were observed to decrease the viscosity of the blend in a systematic fashion. The densities of the materials are higher than that of other types of commercially made foam products; however, they are in the range of similar processes. Finally, it was shown that these cellular materials can be modified to include novel bilayered composite materials composed of a cellular core with an integral skin material.

3M and Radcure are gratefully acknowledged for providing the chemicals used in this study.

REFERENCES

1. J. R. Allaway, D. R. Bloch, and M. P. Fischer, U.S. Pat. 4,378,278 (1983).
2. M. R. Clines and R. A. Findlay, U.S. Pat. 3,484,352 (1969).
3. S. Minomi, Y. Shinke, A. Saito, and A. Osakada, U.S. Pat. 3,709,806 (1973).

4. R. C. Schisler and R. E. Downey, U.S. Pat. 4,767,793 (1988).
5. R. C. Schisler and R. E. Downey, U.S. Pat. 4,771,078 (1988).
6. M. R. Clines and R. A. Findlay, U.S. Pat. 3,484,352 (1969).
7. N. Uejikkoku and M. Takeda, U.S. Pat. 5,110,842 (1992).
8. S. Minomi, Y. Shinke, A. Saito, and A. Osakada, U.S. Pat. 3,709,806 (1973).
9. Y. Shikinami, R. Kimura, Y. Yoshikawa, K. Iida, and K. Hata, U.S. Pat. 4,144,153 (1979).
10. J. C. Goswami and A. J. Yu, U.S. Pat. 4,187,159 (1980).
11. R. C. Schisler and R. E. Downey, U.S. Pat. 4,767,793 (1988).
12. J. R. Allaway, D. R. Bloch, and M. P. Fischer, U.S. Pat. 4,378,278 (1983).
13. D. C. McHerron and G. L. Wilkes, *J. Appl. Polym. Sci.*, **42**, 1045 (1991).
14. J. R. Allaway, D. R. Bloch, and M. P. Fischer, U.S. Pat. 4,378,278 (1983).
15. R. C. Reid, J. M. Prausnitz, and T. K. Sherwood, *The Properties of Gases and Liquids*, 3rd ed., McGraw-Hill, New York, 1977.
16. V. M. Lobe, M.S. thesis, University of Rochester, Rochester, NY, 1973.
17. L. J. Gibson, and M. F. Ashby, *Cellular Solids, Structure and Properties*, Pergamon Press, Oxford, U.K., 1988.

Received January 29, 1996
Accepted March 13, 1996